

MIT Open Access Articles

*Phonostat: Thermostatting phonons
in molecular dynamics simulations*

The MIT Faculty has made this article openly available. **Please share** how this access benefits you. Your story matters.

Citation: Raghunathan, Rajamani, P. Alex Greaney, and Jeffrey C. Grossman. "Phonostat: Thermostatting phonons in molecular dynamics simulations." *The Journal of Chemical Physics* 134, no. 21 (2011): 214117. © 2011 American Institute of Physics

As Published: <http://dx.doi.org/10.1063/1.3597605>

Publisher: American Institute of Physics (AIP)

Persistent URL: <http://hdl.handle.net/1721.1/79661>

Version: Final published version: final published article, as it appeared in a journal, conference proceedings, or other formally published context

Terms of Use: Article is made available in accordance with the publisher's policy and may be subject to US copyright law. Please refer to the publisher's site for terms of use.



Phonostat: Thermostatting phonons in molecular dynamics simulations

Rajamani Raghunathan, P. Alex Greaney, and Jeffrey C. Grossman^{a)}

Department of Materials Science and Engineering, Massachusetts Institute of Technology, 77 Massachusetts Avenue, Cambridge, Massachusetts 02139, USA

(Received 1 February 2011; accepted 17 May 2011; published online 7 June 2011)

Thermostat algorithms in a molecular dynamics simulation maintain an average temperature of a system by regulating the atomic velocities rather than the internal degrees of freedom. Herein, we present a “phonostat” algorithm that can regulate the total energy in a given internal degree of freedom. In this algorithm, the modal energies are computed at each time step using a mode-tracking scheme and then the system is driven by an external driving force of desired frequency and amplitude. The rate and amount of energy exchange between the phonostat and the system is controlled by two distinct damping parameters. Two different schemes for controlling the external driving force amplitude are also presented. In order to test our algorithm, the method is applied initially to a simple anharmonic oscillator for which the role of various phonostat parameters can be carefully tested. We then apply the phonostat to a more realistic (10,0) carbon nanotube system and show how such an approach can be used to regulate energy of highly anharmonic modes. © 2011 American Institute of Physics. [doi:10.1063/1.3597605]

I. INTRODUCTION

Molecular dynamics (MD) simulations are often performed within the canonical ensemble (keeping the number of particles (N), volume (V), and the temperature (T) of the system conserved) in order to mimic experimental conditions. For constant temperature MD simulations, a number of thermostat algorithms have been developed to maintain an average desired temperature. These thermostats range from the most simple (and unphysical) velocity scaling algorithm, to more sophisticated velocity scaling methods such as that proposed by Berendsen,¹ to algorithms that are capable of reproducing the correct canonical ensemble (although not without drawbacks) such as Nose-Hoover² and Langevin³ thermostats. All these thermostats are designed for regulating the average temperature of the system during the simulation, by controlling the atomic velocities rather than the more meaningful internal degrees of freedom.⁴ A traditional thermostat can also be used to excite a single atom; however, a single atom does not represent a thermodynamic ensemble, and the purpose of using a thermostat for a single atom while quite functionally acceptable is not the intended goal of thermostats.⁵ It should also be noted that thermostating a single atom which has 3 degrees of freedom, is still very different from regulating a *single* vibrational eigenmode in which the kinetic energy must go identically to zero twice every oscillation.

The idea to develop a *phonostat* algorithm is motivated by a number of physical processes that involve excitation of only one or several vibrational degrees of freedom, as opposed to the full Boltzmann distribution, thereby creating an unequal energy distribution among various vibrational modes. These phenomena, such as in the excitation of vibrational

modes of molecules, are increasingly accessible experimentally, e.g., in microwave heating, the recently demonstrated carbon nanotube (CNT) radio, and induced surface waves in nanoelectromechanical systems.^{6–8} In order to access and further understand such processes it is desirable to be able to regulate a *single* vibrational mode in a system rather than a collective energy of a multitude of modes. Since the usual thermostat algorithms in MD couple to all degrees of freedom equally, the internal modes are highly coupled and the energy is always distributed among various vibrational degrees of freedom. Hence, a new approach that can excite a given mode with frequency ω and regulate its total energy to some E_{target} is needed.

Of course, without any thermostat, it is possible to excite a mode to an energy E_{target} by assigning initial atomic velocities along the eigen direction. The decay of the excited mode can then be studied by projecting the instantaneous atomic velocities and displacements onto the normal modes of the system.^{9–12} This method is necessarily transient; once perturbed, the mode under investigation receives no additional external excitation. It is also possible to drive a mode by using a velocity scaling technique.¹³ Here, the mode is excited to some energy E_{target} by assigning initial atomic velocities along the eigen direction and the mode velocity is rescaled every time step until equilibrated. Similar to the conventional velocity scaling technique, this method also needs to be turned off once the system is equilibrated. In contrast, many physical processes are continuously driven and therefore require that the mode is driven while simultaneously studying the dissipation of the excited mode. Hence, we seek an algorithm that will allow continuous excitation or driving of one or more vibrational modes. This algorithm could not only be used as a thermostat for a given degree of freedom, but also can provide a method of constraint within the MD simulation to study non-equilibrium phenomena, by regulating an athermal phonon population, quenching activity of

^{a)} Author to whom correspondence should be addressed. Electronic mail: jcg@mit.edu.

particular modes, or for heating soft directions in accelerated dynamics.

In this paper, we present a *phonostat* algorithm to regulate the total energy in a chosen vibrational mode of frequency ω . The phonostat relies on two distinct parts: a mode-projecting scheme that projects the atomic displacements and velocities onto the normal modes to obtain mode velocities and amplitudes, and an energy regulating scheme that regulates the total energy of one or more chosen vibrational modes. In Sec. II we discuss these steps and examine two schemes for regulating the energy based on a driven damped harmonic oscillator. The algorithms are demonstrated by phonostatting a test system of an oscillator coupled to a heat bath. In Sec. III, the use of the phonostat in a more complex MD simulation in which the radial breathing mode of a CNT is driven, while simultaneously measuring its quality factor.

One important feature of the energy regulating part that makes it stand apart from conventional thermostats is that one is regulating a single oscillator rather than an ensemble of oscillators, and as such a different approach is required. Typically thermostats measure and respond to the instantaneous temperature of a group of atoms. For a single oscillator the instantaneous kinetic energy does not provide a good estimate of the average vibrational energy. On the other hand, an approach that regulates the total energy of the mode will drive the system in a controlled manner, without fighting the natural oscillations of the system.

II. METHODOLOGY

Our approach to phonostatting a vibrational mode consists of three steps (Fig. 1): (1) obtaining the normal modes of the system, (2) tracking the total vibrational energy in a given mode during the course of the MD simulation, and (3) driving a mode of frequency ω and simultaneously regulating its total energy, which we refer to as the phonostat (Fig. 1). The first step is a preprocessing step, that is, the normal modes are obtained for the ground state geometry. There is no reason why mode projection cannot be computed with instantaneously computed normal modes, with the Hessian continuously updated using Hessian inference.^{14,15} The only limitation would be additional computational expense. Similarly it is not nec-

essary to drive normal modes of the system. Steps 2 and 3 are carried out sequentially at every time step during the MD run.

A. Computing normal modes

In step 1, we compute the normal modes of the system by constructing the $3N \times 3N$ Hessian or the force constant matrix, for the ground state geometry by the frozen phonon method,

$$k_{ij} = -\frac{f_i(q_i + he_j) - f_i(q_i - he_j)}{2h}, \quad (1)$$

where, k_{ij} is the Hessian matrix element, \hat{e}_j is the unit vector along the direction j , h is the magnitude of displacement, i is the atom index, and q corresponds to the x , y , and z directions. The force f_i in the above equation is given by

$$f_i = -\frac{\partial V}{\partial q_i}, \quad (2)$$

where, V is the interatomic potential. The Hessian matrix is transformed into mass-weighted coordinates and then diagonalized to obtain the normal modes (η) and their corresponding frequencies ν . While for molecules such as water or methane these eigenmodes correspond to the normal modes of vibration, for extended systems such as carbon nanotubes and solids these correspond to the various phonon modes.

B. Mode tracking

In step 2 of our phonostat algorithm, we track the energy of each vibrational mode in the system using a mode-tracking scheme developed previously.¹⁶ In this approach, the energy in the n^{th} vibrational mode at any given instant t is given by

$$E_n(t) = \frac{1}{2}\kappa_n a_n^2(t) + \frac{1}{2}\dot{a}_n^2(t), \quad (3)$$

where, κ_n is the stiffness of the n^{th} vibrational mode, $a_n(t)$ and $\dot{a}_n(t)$ are its instantaneous modal displacement and velocity, respectively. The instantaneous displacement and velocity of mode n are obtained by projecting the atomic positions (q_i) and velocities (\dot{q}_i) onto the eigenvectors of mode η_n after carefully mapping the system onto the reference frame in which

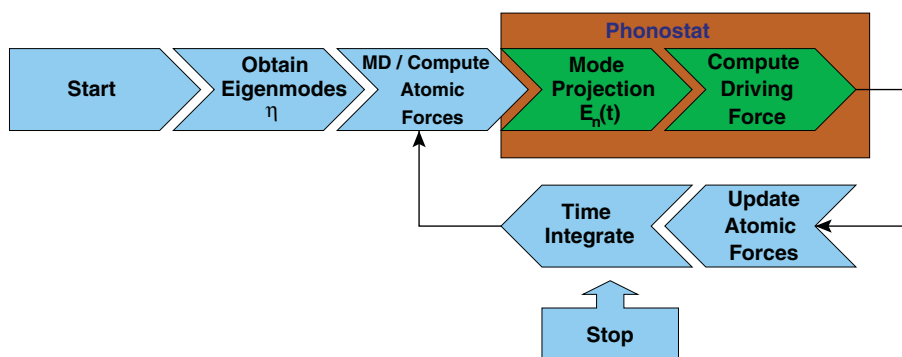


FIG. 1. Schematic of methodology of the phonostat algorithm. Obtaining phonon modes of the system is a separate MD simulation and is performed prior to phonostatting. Steps represented within the rectangle constitute the phonostat and are performed during the course of the simulation.

the phonon modes were obtained in step 1 (Eq. (4)),

$$\begin{aligned} a_n(t) &= \sum_{i=1}^N \sum_{q=xyz} (q_i(t) - q_i(0)) \cdot \eta_{ni}^q, \\ \dot{a}_n(t) &= \sum_{i=1}^N \sum_{q=xyz} q_i(t) \cdot \eta_{ni}^q. \end{aligned} \quad (4)$$

In our earlier implementation of this mode-tracking scheme, these quantities were computed after the full MD simulation, as a post-processing technique.¹⁶ However, for the phonostat algorithm, we now require modal displacements and velocities to be computed on the fly so that the total energy can be regulated. For consistency, the instantaneous kinetic energies of all the modes thus obtained are averaged over the degrees of freedom and verified against the instantaneous temperature of the system at each time step of the MD simulation.

C. The phonostat

The aim of the phonostat is to maintain the energy of the oscillator at some desired target energy E_{target} , different from that of the thermal background (E_T), with some characteristic response time, τ with which it reacts to perturbations of the system. One important aspect of the phonostat that makes it stand apart from ordinary thermostats is that one is regulating a single oscillator rather than an ensemble of oscillators, and as such a different approach is required. Conventional thermostats measure and respond to the instantaneous temperature of a large group of atoms. This averaging ensures that the instantaneous kinetic energy is a reasonable representation of the true thermal energy. The case of a single oscillator is pathological: the instantaneous kinetic energy must oscillate and so does not provide a good estimate of the average vibrational energy. Any energy regulating scheme that reacts only to the kinetic energy will fight the natural oscillations of the system. In this regard some established thermostatting algorithms are better than others. For example the Nosé Hoover (NH) approach uses an inertial extended variable which acts to smooth the response of the thermostat to short time fluctuations. In principle such inertial extended variable approaches could be used as the energy-regulating component of the phonostat, provided the coupling time is sufficiently long; however, there is a fundamental difference in the purpose of thermostats versus the phonostat. The NH thermostat was developed to enforce the same *equilibrium* ensemble averaging as occurs in the canonical ensemble; the phonostat in contrast is a tool for driving a system *away* from equilibrium in a controlled way.

With this philosophical difference in mind we present a different approach to regulating energy that is based on the driven-damped-harmonic oscillator, an approach that more closely resembles many experimental processes and which reflects the non-equilibrium nature of the phonostat. Mimicking an external oscillating driving force, we drive the chosen mode with sinusoidal force with amplitude $f_A(t)$ at frequency ω_P . To dampen fluctuations in the vibrational energy, and to

control the response time of the energy regulating scheme we include a fictitious drag that is parameterized by the dimensionless term ζ_{P1} . Combining these two terms, the force that the phonostat exerts on the mode it is regulating is written as

$$f_P(x, \dot{x}, t) = f_A(t) \cos(\omega_P t + \phi_P) - 2m\omega_P \zeta_{P1} \dot{x}, \quad (5)$$

where ϕ_P is an arbitrary phase term. The phonostat forces the mode to vibrate with frequency ω_P which need not be the natural frequency of the driven mode. In general, we choose $\omega_P = \omega$. However by tuning ω_P one can measure the frequency of a mode and the anharmonic shift in the mode's frequency as it is excited.

In the scheme given in Eq. (5), the energy in the phonostatted mode is regulated by the balance of work done by the driving force and the energy lost due to internal drag. Selecting the parameters $f_A(t)$, and ζ_{P1} such that the desired energy in the mode is obtained, becomes the most critical task. The steady state vibrational energy of a damped harmonic oscillator with mass m and driven at resonance ($\omega_P = \omega$), is related to the steady state driving force amplitude $f_A(0)$ by

$$\begin{aligned} E_{target} &= \frac{1}{2m} \left(\frac{f_A(0)}{2\zeta\omega} \right)^2, \\ f_A(0) &= 2\zeta\omega\sqrt{2mE_{target}}. \end{aligned} \quad (6)$$

This relationship would allow us to set the driving force amplitude required to maintain a desired target energy E_{target} where the damping term, $\zeta = \zeta_{P1} + \zeta_T$, is the total damping on the driven mode and includes the damping that is inherent in the system, ζ_T . This term is the natural dissipation within the system by which fluctuations decay to equilibrium, and in general it is *unknown* and not necessarily constant. The damping terms in ζ are dimensionless with a value of 0 giving no damping and $\zeta = 1$ being the critical damping limit beyond which the oscillator is over damped. One way of minimizing the error in the target energy is to make the fictitious phonostat damping extremely large so that $\zeta_{P1} \gg \zeta_T$. This means that while the value of ζ_T is unknown it must be less than one, and thus to be sure of making this contribution to the total damping negligible one must set $\zeta_{P1} > 1$, that is, setting the phonostat to over damp the system. Over damping the system is not desirable: in developing the phonostat we have set out to preserve the oscillatory dynamics of a vibrational mode, but by setting $\zeta_{P1} > 1$ one quashes these dynamics defeating the aim of the phonostat and making the driven mode numb to the rest of the molecular system.

Rather than setting the phonostat damping to be large from the start and then not adjusting it, one could make an initial guess for the force amplitude for a given ζ_{P1} and then fine tune the force amplitude as the simulation progresses, based on the deviation of the oscillator's energy from the target energy, $E(t) - E_{target}$. The problem is now one of a feedback control system for which many robust procedures have been developed for regulating systems as diverse as furnace thermostats to ships' rudder angles. The most ubiquitous approach is the well known proportional-integral-derivative control where the change in control parameters is dependent on the size of the error (P), how long the error has been this way (I), and how quickly the error is changing (D). For tuning

the phonostat parameters in MD simulations proportional-integral-derivative control is not the most suitable form of feedback as the integral term requires the computer to store the thermal history of the mode in memory and breaks time reversal symmetry of the dynamics. Moreover, the strength of proportional-integral-derivative control is that the system may be treated as a “black box”; however, doing so would throw away what we know about vibrational modes in MD. Instead, our approach is to use a less sophisticated feedback control scheme that is specific to vibrating systems. There are many ways that this can be done; here we present just two schemes both of which adjust only the driving force amplitude, $f_A(t)$. Both of these feedback mechanisms treat $f_A(t)$ as an extended variable in the system’s dynamics, with the simplest case (feedback scheme I) scaling the rate of $f_A(t)$ ($\dot{f}_A(t)$) and the other (feedback scheme II) including an inertial term of $f_A(t)$ ($\ddot{f}_A(t)$).

1. Feedback scheme I

The simplest form of feedback control of $f_A(t)$ is to make the rate of change of force amplitude proportional to the deviation from the target energy. An initial guess of the driving force amplitude is chosen, which in this example is the force that would maintain the target energy if there were no system damping and obtained from Eq. (6),

$$f_i = f_A(0) = 2\zeta_{P1}\omega\sqrt{2mE_{target}}. \quad (7)$$

This is an underestimate of the required driving force due to the presence of internal damping in the system. Hence, the initial guess for the force is corrected by giving a velocity to the force in the form of viscous drag,

$$\dot{f}_A(t)dt = f_A(0)(2\gamma\omega)\left(\frac{E_{target} - E(t)}{E_{target}}\right)dt, \quad (8)$$

where the drag coefficient γ sets how quickly the force corrects itself and is a dimensionless quantity. The energy term $E(t)$ in this expression is the total instantaneous vibrational energy in the mode, that is the sum of the potential and kinetic contributions.

The phonostat has two time scales that can be understood by considering the limiting cases of the system dynamics. Any driven damped harmonic oscillator has a time scale over which transient oscillations decay as the system settles into its steady-state motion. This transient time scale is set only by the total damping of the mode, with $\tau_1 = 1/\omega(\zeta_T + \zeta_{P1})$ being the time for one decrement of e^{-1} of its initial value. This is the time taken for the system to come back into dynamic equilibrium with the driving force after a perturbation in the energy or phase of the driven mode. A second longer time scale, τ_2 , is the time it takes for the driving force amplitude to be tuned to bring the modal energy to the target value. Assuming that the limiting case that the system remains in steady state with the driving force as $f_A(t)$ is adjusted, then the time taken for the error in the energy, $(E_{target} - E(t))$, to be reduced is

$$\tau_2^I = \frac{m(\zeta_T + \zeta_{P1})\sqrt{2A}}{f_A(0)\gamma\sqrt{mE_{target}}}, \quad (9)$$

with A being a parameter of order unity that depends weakly on size of the initial error in the energy. Using this expression one can choose the drag term $\gamma = 2(\zeta_{P1})\omega/f_A(0)\tau_g\sqrt{2m/E_{target}}$, so that the rise time depends on the guessed rise time τ_g and the ratio of the imposed drag, and the system damping $r_\zeta = \zeta_T/\zeta_{P1}$, so that $\tau_2^I \approx (1 + r_\zeta)\tau_g$.

It can be seen that both the time constants are dependent on the unknown term ζ_T . Moreover, if the system is perturbed by the addition of energy into the phonostated mode the response time is given by τ_1 ; on the other hand if the dissipative behavior of the rest of the thermal bath changes then the phonostat responds on the slower time scale τ_2^I . Finally care must be taken to ensure that $\tau_2^I/\tau_1 = \zeta_{P1}(r_\zeta + 1)^2 \gg 1$, so that the phonostat does not try to change the energy of a mode that is out of steady state motion by changing the driving force amplitude.

2. Feedback scheme II

An alternative feedback scheme for tuning the driving force amplitude that incorporates an inertial term in the time evolution of $f_A(t)$ can be used. The idea is based on a critically damped oscillator and is widely used in feedback amplifiers to minimize rise time; since critical damping allows the fastest energy decay in a damped system without overshoot. The displacement x in a damped harmonic oscillator has the equation of motion: $\ddot{x} = -\omega^2x - 2\zeta\omega\dot{x}$, which is critically damped when $\zeta = 1$ giving a decay time $2\pi/\omega$. Mapping the force feedback problem onto this equation gives

$$\ddot{f}_A(t) = -\left(\frac{2\pi}{\tau_g}\right)^2 K(\sqrt{E_{target}} - \sqrt{E(t)}) - \frac{4\pi\zeta_{P2}}{\tau_G}\dot{f}_A(t), \quad (10)$$

where K is a proportionality constant that we have to choose. The above equation has the solution,

$$f_A(t) = f_{target} - (f_{target} - f_A(0))e^{-\zeta_{P2}2\pi t/\tau_g} \times \left(\cos(vt) + \frac{\zeta_{P2}2\pi}{\tau_g v} \sin(vt)\right), \quad (11)$$

with $v = 2\pi/\tau_g\sqrt{K/2(\zeta_T + \zeta_{P1})\omega - \zeta_{P2}^2}$. As with feedback scheme I, we choose the unknown proportionality constant by setting the system damping to zero, $K = 2\zeta_{P1}\omega\sqrt{2m}$. Setting $\zeta_{P2} = 1$ gives

$$f_A(t) = f_{target} - (f_{target} - f_A(0))e^{-2\pi t/\tau_g} \times \left\{ \cosh\left(\frac{2\pi t}{\tau_g}\sqrt{\frac{r_\zeta}{1+r_\zeta}}\right) + \sqrt{\frac{1+r_\zeta}{r_\zeta}} \sinh\left(\frac{2\pi t}{\tau_g}\sqrt{\frac{r_\zeta}{1+r_\zeta}}\right) \right\}. \quad (12)$$

A response time can be estimated from the reciprocal of the gradient in $f_A(t)$ at its steepest point, that has the approximate form $\tau_2/\tau_g \Pi \approx (1 + \sqrt{2})^{\sqrt{2}}/\pi\sqrt{2} - (1 + \sqrt{2})^{\sqrt{2}}(3\sqrt{2} - 2\text{arccosh}(\sqrt{2}))/8\pi(r_\zeta - 1)$.

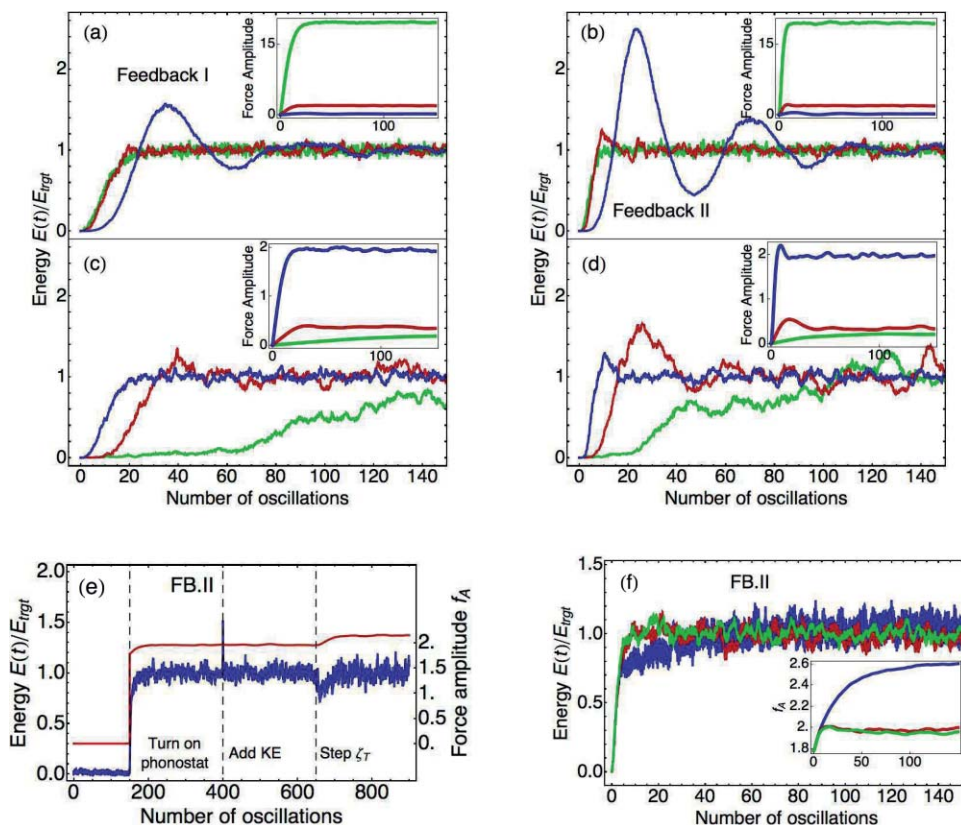


FIG. 2. Plots (a) and (b) show the phonostatted heating of a harmonic oscillator that initially has energy $E(0)/E_{target} = 0.01$ and is in equilibrium with a thermal bath. The force tuning schemes feedback I and feedback II are used in plots (a) and (b), respectively. In both cases heating is shown for the same damping ratio $r_\zeta = 0.1$, with the coupling to the thermal bath being $\zeta_T = 0.001, 0.01$, and 0.1 for the blue, red, and green plots, respectively. The inset plots show the value of the phonostat's driving force, f_A as it is being tuned in each case. Simulations were integrated numerically using the velocity Verlet method with a time step of 10^{-3} of the oscillator's period. Plots (c) and (d) show heating of an oscillator with the same ("unknown") bath damping $\zeta_T = 0.01$ and choices for the fictitious phonostat drag of $\zeta_{p1} = 0.1, 0.01$, and 0.001 for the blue, red, and green plots, respectively. Plot (e) shows the energy in the oscillator (blue) and phonostat's driving force (red) responding to a variety of perturbations. Initially the oscillator is only coupled to the Langevin bath. After 150 oscillations the phonostat is turned on (using feedback II). After 400 oscillations the oscillator is given an extra $E_{target}/2$ of energy in the form of an instantaneous velocity increase. After 650 oscillations the damping from the thermal bath, ζ_T , is increased. Plot (f) shows the energy of a harmonic oscillator (blue) and an asymmetrically anharmonic oscillator (red), and a symmetrically stiffening anharmonic oscillator (green) phonostatted. It can be seen that the harmonic approximation of the potential energy results in a small systematic offset from the target energy.

3. Testing energy regulating schemes

In order to provide a controlled test of this energy regulating portion of the phonostatting algorithm and the feedback schemes, we simulate the simple test system of a single anharmonic oscillator of mass, m . To mimic the strong coupling between various vibrational modes, encountered in a complex atomistic simulation, the oscillator is coupled to a Langevin thermal bath. The equation of motion for the test oscillator is

$$m\ddot{x} = -\frac{d\phi(x)}{dx} - f_T(x, \dot{x}) - f_P(x, \dot{x}, t), \quad (13)$$

with $-d\phi(x)/dx$ being the force from the oscillator potential, and f_T and f_P the external forces from the Langevin thermostat and the phonostat, respectively. We define the potential that the oscillator moves in as $\phi(x) = m\omega^2(x^2/2 + \alpha x^3/3 + \beta x^4/4)$, with ω being the frequency of the oscillator (in the low excitation limit) and α and β the first asymmetric and symmetric anharmonicities. The thermal bath is defined by two parameters: the temperature of the bath E_T , and the dimensionless coupling strength ζ_T , so that $f_T(x, \dot{x}) = -2m\omega\zeta_T\dot{x} + 2\omega\zeta_T\sqrt{2mE_T}\eta(t)$ (where $\eta(t)$ is an

uncorrelated random noise term $\langle\eta(t)\rangle = 0$, and $\langle\eta(t)\eta(t')\rangle = \delta(t - t')$).

Working with this test model we first thermalize the single oscillator system to an initial energy $E(0)$ with the thermostat and then turn on the phonostat to raise the energy of the oscillator to E_{target} . Plots of the system energy versus number of oscillations are shown in Fig. 2, with the inset plots showing the evolution of the phonostat driving force amplitude in each case. Plots (a) and (b) show phonostatting of oscillators with different intrinsic quality factors—that is, with differing strength of coupling to the Langevin bath—but the same damping ratio r_ζ . It can be seen that in both feedback schemes when the fictitious phonostat damping is small τ_1 becomes comparable to τ_2 and the feedback scheme overcompensates the driving force before the oscillator has come into steady-state with the driving force. The inset plots show the feedback scheme tuning the driving force amplitude to different overall values to balance the different drag strengths. Figures 2(c) and 2(d) show results of simulations with the same internal damping ζ_T with differing phonostat damping. This test represents how one might approach a real MD sim-

ulation in which the intrinsic damping of the phonostatted mode ζ_T is unknown. The three sets of data show the cases when the phonostat damping is dominant, when the phonostat damping and intrinsic damping are comparable, and when the intrinsic damping dominates. In this latter case the feedback time τ_2 becomes very long, and one would have to increase the damping of the phonostat. Plots (a)–(d) in Fig. 2 show little advantage of one feedback mechanism than the other. In both cases some adjustment is needed in order to set the phonostat damping appropriate for the system as the two time scales inherent in the problem are controlled separately by the total damping and the damping ratio. This can be seen in Fig. 2(e) in which the response of the phonostatted system to perturbations is shown. After 400 oscillations extra energy is added to the oscillator raising it above the target energy. The energy is corrected in time scale τ_1 without a change in the driving force amplitude. After 650 oscillations the strength of the coupling of the oscillator to the thermal bath is increased. The phonostat responds over time scale τ_2 , increasing the driving force amplitude to match the increased damping. The last plot in Fig. 2, plot (f), shows the results of phonostatting anharmonic oscillators. In the feedback schemes in Eqs. (8) and (10) the instantaneous energy $E(t)$ is the sum of the exact kinetic energy and the harmonic *approximation* for the potential energy. For an anharmonic potential this will result in a small systematic error in $E(t)$ that will result in the mode being on average shifted from the target energy. Plotted in Fig. 2(f) is the *exact* total energy of the oscillator and it can be seen that average energy of the anharmonic oscillators is subtly shifted from that of the harmonic oscillator. This error can be simply corrected by scaling the target energy by the fractional error in the average energy estimate. Together the plots in Fig. 2 show that the phonostat scheme works well at maintaining the oscillator energy at the target energy and the schemes are robust with respect to the choice of phonostat parameters.

III. PHONOSTATTING A (10,0) CARBON NANOTUBE

Our original motivation for developing the phonostat algorithm was to understand the large intrinsic dissipation observed in driven CNT resonators. CNTs are remarkable structures that due to their extreme stiffness to mass ratio and the string-like shape make them attractive candidates for use as the resonating members in nanoelectromechanical devices.^{6,17–20} CNT resonators can be readily integrated with traditional electronics and the resonators can be both driven and sensed electronically. These resonators can have frequencies in the GHz range, making them useful for applications in mass and chemical sensing, wireless communications, and signal processing. The largest impediment to the ubiquitous use of CNT resonators is their poor quality factor. The quality factor (Q) is a measure of dissipation within a system and is given by the relation,

$$Q = 2\pi \times \frac{\text{Energy stored}}{\text{Energy dissipated per cycle}}. \quad (14)$$

While the phonostat by itself is insufficient to simulate a driven resonator (one also requires a method of remov-

ing heat from the system without disturbing the dynamics of the driven mode—a matter that will be addressed in a separate forthcoming article), the CNT remains a good test system to demonstrate the capability of the phonostat algorithm. CNTs have a well understood and systematic structure, and they are also strongly dissipative, and possess both symmetric and asymmetric anharmonic modes. The CNT can be modeled with the AIREBO empirical potential²¹ which treats both the anharmonic C-C covalent bond, and the longer range dispersive interactions switching smoothly between them as a function of spacing and local coordination. String-like resonators (of which the CNT is an example) become nonlinear at relatively modest excitations due to the elongation in overall length as the mode flexes. In addition to these symmetrically stiffening modes of the CNT there are modes, such as the radial breathing mode that soften in one direction but stiffen in the other. These asymmetric anharmonic modes (where the third order term in the potential energy surface dominates over the 4th order term) couple strongly to modes with half the vibrational frequency.¹⁶ Using this well understood system we show that we can drive the breathing mode with the phonostat—regulating its energy—causing the heating of modes with exactly half the frequency of the breathing mode—leading to thermalizing the tube.

There are a few added advantages of using our phonostat algorithm while simulating such continuous driving conditions. First, the quality factor (Q) can be computed directly while simultaneously driving a mode. When the phonostat and the system are in equilibrium, the work done by the phonostat must be equal to the change in the total energy of the phonostatted mode. Thus, Q can be obtained directly from the power input by the phonostat (Eq. (15)) assuming that the rate of accumulation of energy in the driven mode is negligible in comparison to that dissipated by the mode,

$$Q = 2\pi\nu \times \frac{\text{Energy stored}}{\text{Power delivered by phonostat}}. \quad (15)$$

However, this approximation is not valid during the initial steps of the simulation when the mode is being brought into equilibrium with the phonostat. Finally, the algorithm can also be used to clamp modes by canceling the forces of atoms along a given normal mode direction to identify pathways of heat dissipation.

In order to phonostat a phonon mode of a carbon nanotube, the method is integrated into the LAMMPS molecular dynamics code.²² Before phonostatting the radial breathing mode of a (10,0) carbon nanotube containing 800 atoms, the normal modes of the system and their corresponding frequencies are obtained using the frozen phonon method, as discussed in Sec. II A. In this system, there are 2400 normal modes in total, of which the first four correspond to translational and rotational degrees of freedom. The remaining 2396 modes are the various phonon modes of the system. MD simulations are performed on the relaxed structure of a (10,0) CNT within the microcanonical ensemble using the AIREBO force-field, with a time step of 0.2 fs and Verlet integration scheme, for a total time of 1 ns.²¹ First the system is prepared at a given background temperature T_{BG} using a langevin

thermostat within a microcanonical ensemble for 50 ps. This ensures that the system is thermalized with a distribution of energy among various phonon modes of the system. We perform two separate simulations corresponding to two different $T_{BG} = 600$ and 300 K, respectively. In each of these simulations, using the eigenmodes (η_n) and frequencies (ω_n) we first compute the total energy $E_n(t)$ of each mode at a given time t using the mode tracking algorithm (Eqs. (3) and (4)). Since we start the simulation with the ground state structure of the CNT, the tube expands radially due to the thermal expansion, when the system is heated to 300 or 600 K. However, the presence of periodic boundary conditions along the length of the tube restricts thermal expansion in this direction. In order to obtain the correct modal displacement $a_{RBM}^c(t)$ of the radial breathing mode, it is necessary to separate out the radial thermal expansion from the instantaneous modal displacement $a_{RBM}(t)$. This is done by obtaining the exponentially weighted moving average of the breathing mode displacements and subtracting this out from the instantaneous displacement (Eq. (16)),

$$S_{t=0} = \alpha a_{RBM}(t=0)$$

$$\left. \begin{aligned} S_t &= \alpha a_{RBM}(t) + (1 - \alpha) S_{t-\delta t} \\ a_{RBM}^c(t) &= a_{RBM}(t) - S_t \end{aligned} \right\} \text{for } t > 0, \quad (16)$$

where α is a coefficient that represents the degree of weighting decrease. S_t is the average at time t , $a_{RBM}(t)$ and $a_{RBM}^c(t)$ are the instantaneous and the corrected breathing mode displacements respectively at time t and δt is the molecular dynamics simulation time step. The value of α can be set between 0 and 1; larger values of α discounts older values of $a_{RBM}(t)$ faster. The value of α is chosen such that the modal displacements are averaged over 10 breathing mode cycles. Then the total energy of the radial breathing mode is obtained from $E_{RBM} = 1/2 k_{RBM} a_{RBM}^c(t)^2 + 1/2 \dot{a}^2(t)$. During the thermalization process the average total energy in the radial breathing mode was about 0.1 meV/atom.

After 50 ps, the langevin thermostat is turned off and the phonostat is applied on the breathing mode with E_{target} set to 0.5 meV/atom. In the phonostat step of our algorithm, though the initial guess f_i for the driving force could be 0 or $f_A(0)$, we have chosen $f_i = 0$. The results presented here are obtained by using feedback scheme I for the force correction.

In Fig. 3(a) we present total energy of the radial breathing mode vs. time, phonostatted to $E_{target} = 0.5$ meV/atom, for $\zeta_{P1} = 0.15$, $\gamma = 0.001$, and the two different background temperatures $T_{BG} = 600$ and 300 K. The driving force amplitude of the phonostat is also plotted as a function of time in Fig. 3(b). We see that for $T_{BG} = 600$ and 300 K, the driving force starts from 0 and increases steadily until the mode reaches E_{target} , as expected. However, the temperature of the entire system, increases monotonically once the phonostat is turned on (Fig. 4(a)). The radial breathing mode that is being driven is highly anharmonic and couples strongly to the half frequency modes and thus dissipates energy into the

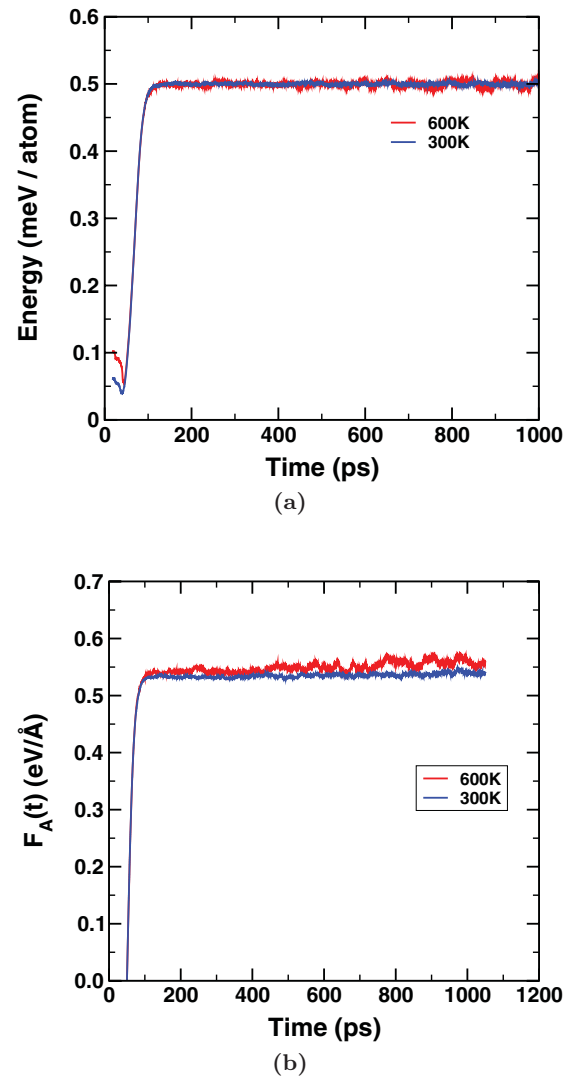


FIG. 3. (a) Total energy and (b) phonostat force amplitude plotted as a function of time of radial breathing mode phonostatted at 0.4 eV (0.5 meV/atom) for $\zeta_{P1} = 0.15$, $\gamma = 0.001$. The red and blue curves correspond to $T_{BG} = 600$ K and 300 K, respectively.

background leading to rise in the total energy of the system and a corresponding increase in the temperature of the tube in both cases. A continuously driven mode will tend to energize the entire system by dissipating until a steady state wherein all the degrees of freedom come into equilibrium with the driven mode is reached; that is, at equilibrium each degree of freedom will have a total energy equal to the driven energy, $E_{target} = 0.5$ meV/atom, corresponding to a system temperature of 4642 K. In our simulations, the temperature of the whole system increased from 600 K to about 1500 K and from 300 to 700 K for $T_{BG} = 600$ and 300 K, respectively, in 1 ns. We also notice that the system heats up faster and becomes more dissipative as the simulation progresses. The increase in the rate of dissipation is also complemented by a gradual increase in the phonostat driving force amplitude. Using the power delivered by the phonostat, we also computed the quality factor of the driven mode as a function of time for both simulations. We have plotted the quality factor of the mode vs. the average temperature of the nanotube in Fig. 4(b).

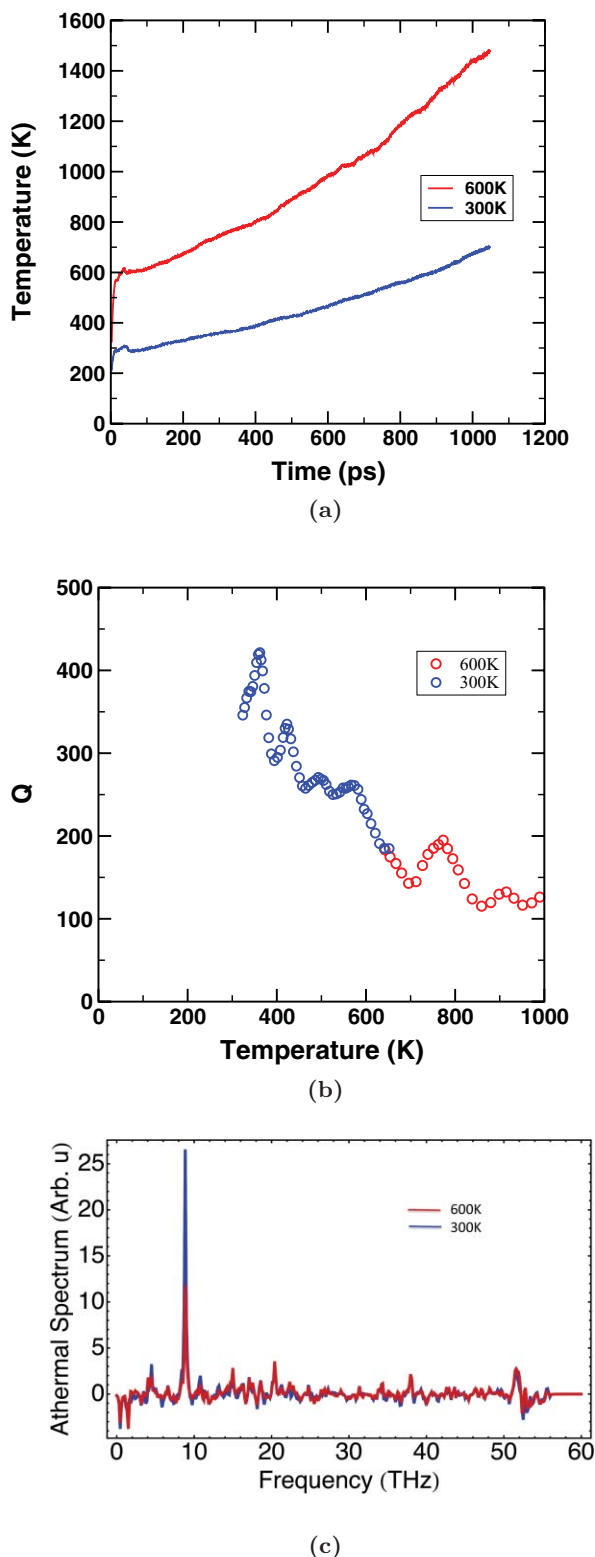


FIG. 4. (a) Background temperature vs. time of the system obtained by averaging kinetic energies over all degrees of freedom, (b) Quality factor of carbon nanotube as a function of temperature with radial breathing mode under continuous driving at $E_{target} = 0.5$ meV/atom. The red and blue circles correspond to simulations with $T_{BG} = 600$ and 300 K, respectively. (c) mean deviation of the normalized mode energies from the (classical) equilibrium filling for $T_{BG} = 600$ (red) and 300 K (blue). In effect this is the athermal excitation of the vibrational modes.

We find that the quality factor of the radial breathing mode decreases with increase in system temperature due to increased dissipation at elevated temperatures. Also computed is the mean deviation from equilibrium of the filling of the vibrational modes—the athermal excitation (Fig. 4(c)). This shows a peak from the mode being driven, but also a series of lesser peaks, including one at half the driving frequency. Though these peaks may look like noise, a closer inspection reveals that there is a very strong correlation between the peaks in simulation sets for $T_{BG} = 600$ and 300 K, indicating that the energy from the driven mode is dissipating into a limited subset of other modes, that are distributed uniformly across the full frequency spectrum of the tube.

IV. CONCLUSIONS

In this paper we presented a generic algorithm to regulate energy in any given internal degree of freedom. Our approach is based on obtaining the instantaneous modal energies using a mode-tracking algorithm and then driving the system using an external force of fixed frequency ω_o and a time varying force $f_A(t)$. We also identified and presented at least two distinct ways of controlling the external driving force for phonostating a mode. Our method is illustrated by a test case of a driven damped harmonic oscillator. Our study shows that the modal energy rise time can be controlled by two parameters, ζ_{P1} and γ . We then continuously drive the radially breathing mode of a (10,0) CNT resonator at two different background temperatures and demonstrate the robustness of the technique even under dissipative conditions. The quality factor of the breathing mode is also computed for different system temperatures from the phonostat power, in a single simulation.

ACKNOWLEDGMENTS

This project received funding from the Defense Threat Reduction Agency-Joint Science and Technology Office for Chemical and Biological Defense (Grant No. HDTRA1-09-1-0006).

- ¹H. J. C. Berendsen, J. P. M. Postma, W. van Gunsteren, A. DiNola, and J. R. Haak, *J. Chem. Phys.* **81**, 3684 (1984).
- ²S. Nosé, *J. Chem. Phys.* **81**, 511 (1984).
- ³R. Kubo, *Rep. Prog. Phys.* **29**, 255 (1966).
- ⁴D. Frankel and B. Smit, *Understanding Molecular Simulation: From Algorithms to Applications* (Academic, New York, 2002).
- ⁵P. H. Nguyen, S.-M. Park, and G. Stock, *J. Chem. Phys.* **132**, 025102 (2010).
- ⁶K. Jensen, J. Weldon, H. Garcia, and A. Zettl, *Nano Lett.* **7**, 3508 (2007).
- ⁷H. G. Craighead, *Science* **290**, 1532 (2000).
- ⁸A. Sampathkumar, K. L. Ekinici, and T. W. Murray, *Nano Lett.* **11**, 1014 (2011).
- ⁹H. Jiang, M.-F. Yu, B. Liu, and Y. Huang, *Phys. Rev. Lett.* **93**, 185501 (2004).
- ¹⁰K. Moritsugu, O. Miyashita, and A. Kidera, *Phys. Rev. Lett.* **85**, 3970 (2000).
- ¹¹S. R. Phillpot, P. K. Schelling, and P. Keblinski, *J. Mater. Sci.* **40**, 3143 (2004).
- ¹²P. A. Greaney, G. Lani, G. Cicero, and J. C. Grossman, *Nano Lett.* **9**, 3699 (2009).
- ¹³L. M. Raff, *J. Chem. Phys.* **89**, 5680 (1988).
- ¹⁴P. H. Nguyen, and G. Stock, *J. Chem. Phys.* **119**, 11350 (2003).
- ¹⁵A. Bastida, M. A. Soler, J. Zúñiga, A. Requena, A. Kalstein, and S. Fernández-Alberti, *J. Chem. Phys.* **132**, 224501 (2010).

- ¹⁶P. Alex Greaney and J. C. Grossman, *Phys. Rev. Lett.* **98**, 125503 (2007).
- ¹⁷M. Bockrath, *Nat. Nanotechnol.* **4**, 619 (2009).
- ¹⁸K. L. Ekinci, M. L. Roukes, *Rev. Sci. Instrum.* **76**, 061101 (2005).
- ¹⁹B. Lassagne, D. Garcia-Sanchez, A. Aguasca, and A. Bachtold, *Nano Lett.* **8**, 3735 (2008).
- ²⁰H.-Y. Chiu, P. Hung, H. W. Ch. Postma, and M. Bockrath, *Nano Lett.* **8**, 4342 (2008).
- ²¹S. J. Stuart, A. B. Tutein, and J. A. Harrison, *J. Chem. Phys.* **112**, 6472 (2000).
- ²²S. J. Plimpton, *J. Comp. Phys.* **117**, 1 (1995), see <http://lammmps.sandia.gov>.